LAWRENCE
LIVERMORE
NATIONAL
LABORATORY

LLNL-PROC-404474

The High-Resolution Lightweight Telescope for the EUV (HiLiTE)

D. S. Martinez-Galarce, P. Boerner, R. Soufli, B. De Pontieu, N. Katz, A. Title, E. M. Gullikson, J. C. Robinson, S. L. Baker

June 5, 2008

Space Telescopes and Instrumentation II: Ultraviolet to Gamma Ray 2008, SPIE Aatronomical Instrumentation
Marseille, France
June 23, 2008 through June 28, 2008

Disclaimer

The High-Resolution Lightweight Telescope for the EUV (HiLiTE)

Dennis S. Martínez-Galarce[1*], Paul Boerner[1], Regina Soufli[2], Bart De Pontieu[1], Noah Katz[1], Alan Title[1], Eric M. Gullikson[3], Jeff C. Robinson[2] and Sherry L. Baker[2]

[1]Lockheed Martin Advanced Technology Center, 3251 Hanover Street, Palo Alto, CA 94305, USA
[2]Lawrence Livermore National Laboratory, 7000 East Avenue, Livermore, CA 94550, USA
[3]Lawrence Berkeley National Laboratory, Berkeley, CA 94720, USA

ABSTRACT

The High-resolution Lightweight Telescope for the EUV (HiLiTE) is a Cassegrain telescope that will be made entirely of Silicon Carbide (SiC), optical substrates and metering structure alike. Using multilayer coatings, this instrument will be tuned to operate at the 465 Å Ne VII emission line, formed in solar transition region plasma at ~500,000 K. HiLiTE will have an aperture of 30 cm, angular resolution of ~0.2 arc seconds and operate at a cadence of ~5 seconds or less, having a mass that is about ¼ that of one of the 20 cm aperture telescopes on the Atmospheric Imaging Assembly (AIA) instrument aboard NASA's Solar Dynamics Observatory (SDO). This new instrument technology thus serves as a path finder to a post-AIA, Explorer-class missions.

Keywords: EUV solar physics, silicon carbide, Mg/SiC multilayers

1. INTRODUCTION

The highly-structured and extremely dynamic interface between the photosphere and the corona is of crucial importance in understanding solar activity and space weather. Over 90% of the non-radiative energy going into the outer atmosphere to drive solar activity is dissipated within this region. While directly observing this interface is complicated because of the predominantly optically thick and scattering chromospheric lines, optically thin line emission from the transition region (TR), which is at the top end of the interface, provides access to the dynamics and structuring of the interface region. However, even the most state-of-the-art examples of the current generation of EUV imagers and spectrographs are unable to provide the spatial resolution and cadence necessary to capture the TR, preventing our understanding of coronal heating mechanisms and lower atmospheric topology. Recent advances in multilayer fabrication and lightweight telescope technology offer the possibility to make a major step forward in TR and coronal physics by enabling us to build a very high-resolution, high throughput and lightweight EUV telescope that directly images the TR at 500,000 K. Using such a telescope, we will be able to test and constrain the most recent models of turbulent coronal heating, and obtain a fuller understanding of the topology and dynamics of the low atmosphere than current instruments allow.

We have completed a preliminary design and feasibility demonstration of the High-resolution Lightweight Telescope for the EUV (HiLiTE): a Cassegrain telescope with an aperture of 30 cm, angular resolution of 0.2 arcseconds, and a mass that is about ¼ that of one of the 20 cm aperture telescopes on the AIA instrument aboard SDO. The instrument bandpass will be tuned to the 465 Å Ne VII emission line formed in plasma at 500,000 K. The HiLiTE instrument, including both mirrors and the metering structure, will be constructed entirely from lightweight, thermally stable, high-stiffness advanced Silicon Carbide (SiC) material. While SiC is an extremely promising material for space telescopes, SiC optics with the figure and surface finish required for normal-incidence EUV multilayers have not yet been demonstrated. We have proposed to NASA a three-year technology development effort to fabricate the primary and secondary mirrors of the HiLiTE telescope; to measure their surface figure and roughness in order to determine that they are of suitable quality for high-resolution, high-throughput EUV performance; and to deposit and test the multilayer coatings optimized for normal incidence reflection of the Ne VII emission line at 465 Å. After successful completion of this program, a follow-on proposal will be submitted to integrate the mirrors into the metering structure, integrate the HiLiTE with a suitable focal plane assembly, and fly it on a sounding rocket. By leveraging off the expertise in the ATSSI[1] sounding

* *denmart@lmsal.com*

rocket payload development at the Lockheed Martin Solar and Astrophysics Laboratory (LMSAL) of the Advanced Technology Center (LMATC), the HiLiTE program could be ready for flight by 2013. It will be capable of providing an unprecedented look at the TR; while the MOSES payload was recently funded to study coronal holes at 465 Å with ~1.2 arcsecond resolution[2] HiLiTE will be the first high-resolution, high-cadence, narrowband EUV imager of the solar transition region at 500,000 K. It will provide the highest-resolution EUV images of the solar atmosphere ever taken; and it will take images at a cadence comparable to that of the best space- and ground-based chromospheric imagers.

When flown on a sounding rocket (or a similar telescope on a satellite mission), HiLiTE will provide deep insight into some of the most important issues in solar physics. Its high cadence (~5 sec) and high resolution (0.2 arcsec) imaging of the complex and poorly understood TR will, for the first time, resolve the spatial scale of the dominant driver of all atmospheric activity: magneto-convection on a granular scale (~1 Mm). In addition, the HiLiTE bandpass is dominated by emission from TR plasma at ~500,000 K, which has never before been observed with an instrument that can image at a cadence of order seconds. In this temperature regime, the TR reacts very sensitively to the energy deposition associated with magnetic field reconfigurations or reconnection in the coronal volume, whether caused by flares or CMEs. Thus, a TR imager is an ideal instrument to study a whole range of issues from lower atmospheric topology, coronal heating, reconnection, to particle acceleration.

Just as significantly, this technology development program will address a number of technical challenges standing in the way of the next generation of high resolution, light-weight EUV telescopes that are crucial for future missions such as the Reconnection and Microscale Mission (RAM). Those missions will demand low mass, high throughput (and thus large diameter) EUV telescopes that are thermally and mechanically stable enough to reliably provide high resolution imaging. Simply modifying existing designs – scaling them up to improve throughput and tightening their tolerances to improve resolution – will cause the complexity and cost of future missions to explode. HiLiTE will serve as a pathfinder for the technologies and designs that will enable such large optical systems.

HiLiTE data will provide powerful synergies with the variety of photospheric, chromospheric and coronal observations that will be available over the next five years. By the time HiLiTE will be ready for launch, both the SDO and Hinode will most likely still be active. The AIA instrument on SDO will provide full thermal context of loops from 0.8 to 10 MK, as well as at 0.1 MK. Hinode/SOT provides magnetograms in the low atmosphere as well as chromospheric imaging, which is crucial to study the connection of the TR to the lower atmosphere. EIS provides spectra over a range of temperatures from the corona down to the TR.

2. TECHNICAL APPROACH

2.1 Mechanical and Optical Design

The HiLiTE telescope has been designed to provide the first observations capable of addressing the science questions described above. HiLiTE will employ a two-mirror classical Cassegrain design. The plate scale is set to achieve 0.1 arcsecond pixels for a 5 μm detector pitch, which dictates an effective focal length of 10.3 m. Because we are working in the EUV, refracting optics cannot be used to increase magnification or correct aberrations. Therefore, the effective focal length must be achieved with only the primary and secondary mirrors. Fortunately, the extremely high stiffness of SiC allows us to use a relatively long metering structure to increase the mirror spacing, reducing the magnification and sensitivity to misalignment of the secondary mirror. The HiLiTE design shown in Figure 1 is capable of achieving 0.2 arcsecond spatial resolution through the launch and flight of a sounding rocket without an active focus or alignment mechanism for the secondary. The optical parameters of the design are described in Table 1. The primary and secondary mirrors are both made of SiC. In recent years, it has been demonstrated that lightweight SiC mirror substrates can be polished to aspheric shapes and can provide excellent images[3,4,5]. The LORRI instrument on New Horizons[6] (Conard, 2005) uses an all-SiC, passively athermal 20 cm telescope to produce high-resolution images. Several groups, both within the LMATC and elsewhere at Lockheed Martin, have studied high-quality SiC optics for use in a variety of flight and proto-flight applications. HiLiTE will push this promising technology forward, becoming the first astronomical instrument to achieve sub-arcsecond resolution with a SiC optical system, and the first to use a reflective normal-incidence multilayer on a SiC mirror. Because all the optics and the metering structure are constructed of the same material, the instrument is inherently passively athermal – the curvature of the optics automatically compensates for changes in the mirror spacing to maintain focus under temperature soak conditions. The aluminum focal plane structure gives a small focus sensitivity to bulk temperature change of 1.6 μm/K; with a focus budget of 250 μm, this is not a concern. The small but nonzero CTE of SiC also gives a small sensitivity to temperature gradients; however, gradients

will be minimal thanks to the high thermal conductivity of the material and the entrance filters, which nearly eliminate heat input.

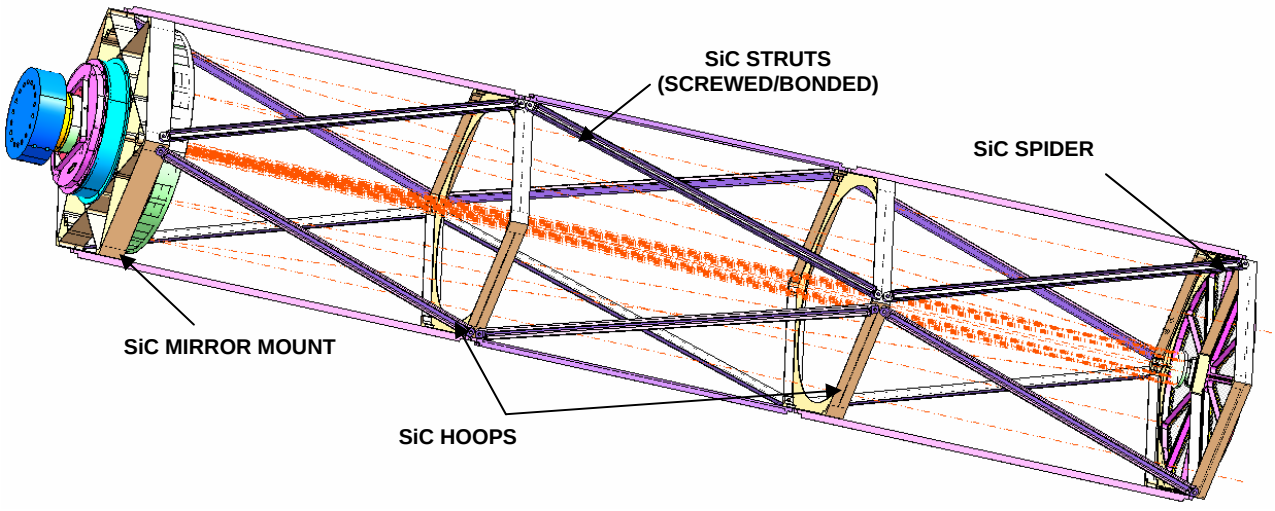

Figure 1. The optical and mechanical design of the HiLiTE features a 30 cm aperture and a 150 cm primary-to-secondary mirror spacing. The metering structure and focal plane assembly will not be fabricated as part of the proposed work.

The telescope structure has been designed to fit inside the existing Multi-Spectral Solar Telescope Array (MSSTA) rocket truss, which flew three times between 1991 and 2002 [7,8]. We conducted finite element analysis of the design in this configuration in order to assess the instrument's performance in a rocket flight; see Figure 2. With simple supports to a rigid interface (the payload truss), and despite the long metering tube, the telescope assembly's first mode frequency is 126 Hz – well above the 50 Hz requirement of the Altitude Control System (ACS). This helps ensure that the alignment will not be affected by launch vibrations, and that the SPARCS guidance system will function properly in flight (see Section 2.3.3.). The primary mirror is extremely light and stiff, with a first mode frequency of nearly 1500 Hz.

	System
Effective Focal Length	10.313 m
Focal Ratio	f/34
Plate Scale	20 arcsec/mm
Field of View	> 4x4 arcmin*
	Primary Mirror
Clear Aperture	300 mm
Radius of Curvature	- 3564.2564 mm
Conic	- 1
	Secondary Mirror
Clear Aperture	40 mm
Radius of Curvature	- 680.89795 mm
Conic	- 2.0116

Table 1: Optical design parameters of the HiLiTE telescope.
* The proposed work does not include the integration of the focal plane and detector, which acts as the field stop for the telescope. However, the optical design is optimized to image over a field of view of at least 4x4 arcminutes.

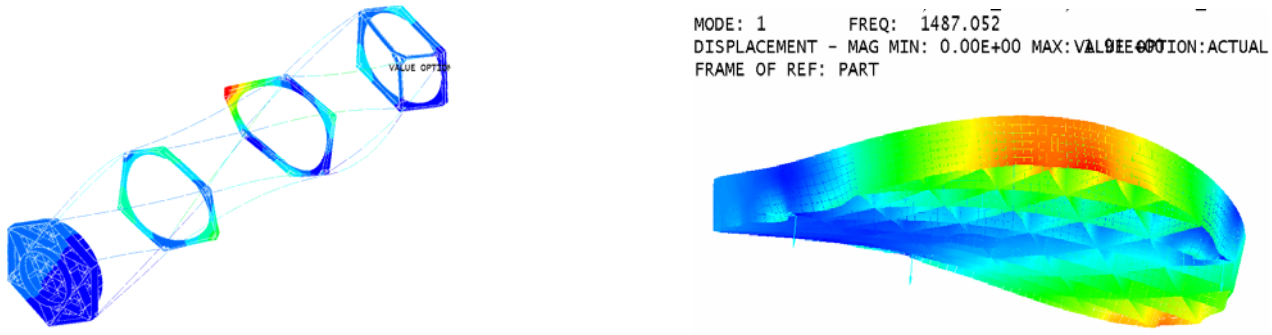

Figure 2. Finite element analysis of the HiLiTE mechanical design with 38K nodes and 40K elements indicate a first mode for the structure at 126 Hz, and a first mode for the primary mirror at 1487 Hz. The SiC structure has ample margin against launch loads.

The telescope is designed to be mounted to the rocket truss via elastomeric isolators chosen to give a resonance at least an octave above the 50 Hz bandwidth of the SPARCS ACS. This will avoid phase lag issues with the ACS sensor mounted on the telescope spider. It also rolls off high frequency structure-borne vibration and reduces stresses, in particular on the entrance filters. The filters also benefit from the evacuated rocket casing, eliminating acoustic pressure stress. In addition to ensuring that the HiLiTE is capable of surviving the thermal and mechanical stress of a rocket launch and still meeting its performance goals, we designed the instrument to minimize mass. For a sounding rocket payload, there is no immediate advantage in cost or observing time in reducing the instrument's mass, given that the payload will use a standard 22" experiment-section skin. However, future satellite missions building on the HiLiTE design will almost certainly be mass-constrained. As designed, the telescope assembly (including both mirrors, but not including the camera/focal plane assembly) has a mass of only 3.9 kg, less than ¼ as much as an AIA telescope assembly at a similar build level – despite the fact that HiLiTE has more than twice the collecting area of an AIA telescope. An even more important design consideration is ensuring that the fabrication, assembly and alignment tolerances are realistic, and that those tolerances can still be met during flight. The SiC struts that make up the HiLiTE telescope truss are screwed and bonded to SiC hoops; the truss assembly tolerances ensure that the mounting surfaces for the primary and secondary mirror cells are coaxial to within 0.040" and parallel to within 0.010". Fine adjustment is performed by lapping pads on the secondary focus/tilt spacer (see Figure 3). Thanks to the stiffness of the structure and the relatively forgiving optical design, the instrument can maintain primary-to-secondary decenter, tip/tilt and defocus within their allocations (see Section 2.3.3).

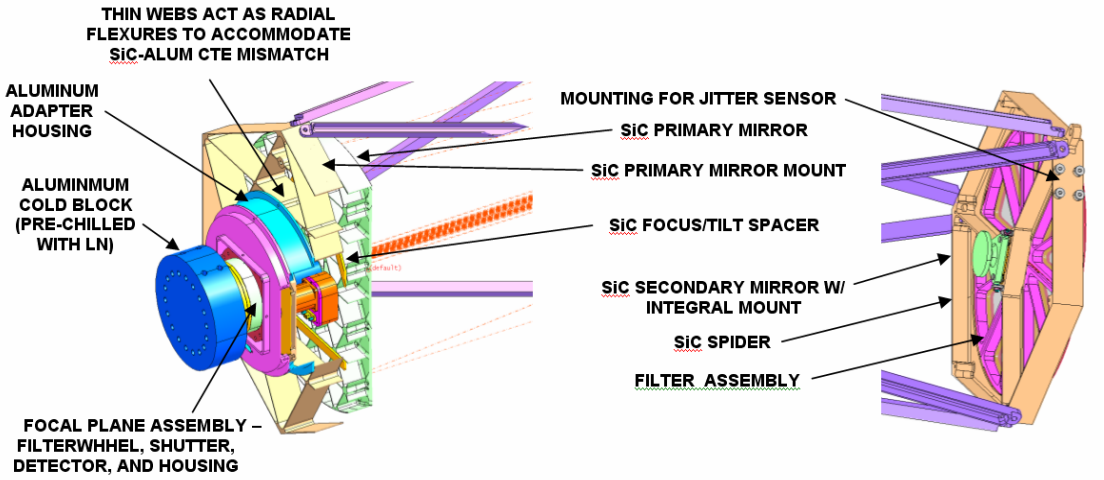

Figure 3: Left: the primary mirror is shown assembled into the telescope structure. The focal plane assembly and struts pictured here will not be built as part of the proposed program. **Right:** the spider and secondary mirror are shown.

2.2 Mirror substrates and multilayer coatings

In an EUV reflective system such as HiLiTE, scattering from the telescope mirrors will result in a loss of throughput and reduced imaging contrast[9]. Roughness with a short spatial period will scatter light at large angles (outside the detector field of view), reducing the reflectivity of the mirrors and causing a loss of throughput. Mid-spatial frequency roughness results in light scattered within the solar image, which reduces image contrast. The relevant spatial frequencies for mid- and high-spatial frequency roughness can be calculated based on the angular scale of the sun and the angular resolution of the instrument, as well as the separation of the primary and secondary mirrors from the focal plane. The relevant scales for the HiLiTE mirrors are listed in Table 2. These throughput and imaging contrast reduction effects are the basic drivers behind the figure and finish specifications for the HiLiTE EUV mirror substrates. As discussed in Ref. 9, the root-mean-square (RMS) roughness in a specific spatial frequency range is determined by the system geometry and the allowable scattering per mirror. Table 3 gives the allowable roughness for 1, 2, and 5% scattered light per mirror surface for the HiLiTE design. In reality, the shortest period roughness can be influenced by smoothing of the multilayer coating, which, for DC-magnetron sputtered coatings relevant to this paper is expected to occur at spatial periods shorter than 0.02 μm[10,11,12]. Nonetheless, it can be a challenging task for mirror manufacturers to achieve the roughness and figure specifications for EUV operation on large-area aspheric mirrors. It is therefore important to characterize the surface topography and to accurately measure the roughness of a substrate prior to multilayer deposition, in order to understand and interpret correctly its reflective performance after multilayer coating.

	Primary Mirror	**Secondary Mirror**
Spatial periods (Λ) relevant to mid-spatial roughness	10 μm < Λ < 20 mm	2 μm < Λ< 3 mm
Spatial periods (Λ) relevant to high-spatial roughness	0.05 μm < Λ < 10 μm	0.05 μm < Λ < 2 μm

Table 2: Spatial periods relevant to high- and mid-spatial frequency roughness for the HiLiTE design

Relative loss / mirror	Roughness σ (nm RMS)
1%	0.37
2%	0.5
5%	0.8

Table 3. Reflectivity loss due to surface roughness.

To evaluate the feasibility of obtaining SiC substrates meeting the above surface finish requirements from commercial polishing vendors, we obtained SiC witness substrates (flat disks ~3" in diameter) from a candidate vendor using two different polishing processes. These coupons were characterized by precision surface metrology at LLNL. Atomic Force Microscope (AFM) measurements were performed over 2×2 μm^2 and 10×10 μm^2 areas at two locations in the center area on each substrate. Prior to metrology, the substrates were cleaned at LLNL with a custom-developed process, consisting of rinsing in a water-based solution followed by drying in N2 environment. This process has been shown to remove polishing residue and contamination from the top surface without degrading the surface finish[13]. The AFM results on one of the substrate locations are shown in Figure 4. Mid-spatial frequency roughness measurements were performed in the spatial frequency range from 7×10^{-6} nm^{-1} to 2×10^{-4} nm^{-1} using a Zygo optical profiling microscope. The power spectral density (PSD) derived from the AFM and Zygo surface metrology results are shown in Figure 5; the computed RMS roughness values obtained from these measurements are shown in Table 4. These results, compared with the guidelines in Table 3, demonstrate that the SiC witness substrate polished by process 1 would achieve less than 1% relative loss (due to scattering) per mirror reflection and the SiC witness substrate polished by process 2 would achieve about 5% relative loss per mirror reflection in the HiLiTE system, in the high-spatial frequency range. The results obtained on flat witness SiC coupons are very promising and indicate that polishing vendor capabilities will be able to produce the large-area, aspheric SiC mirror substrates of the HiLiTE telescope.

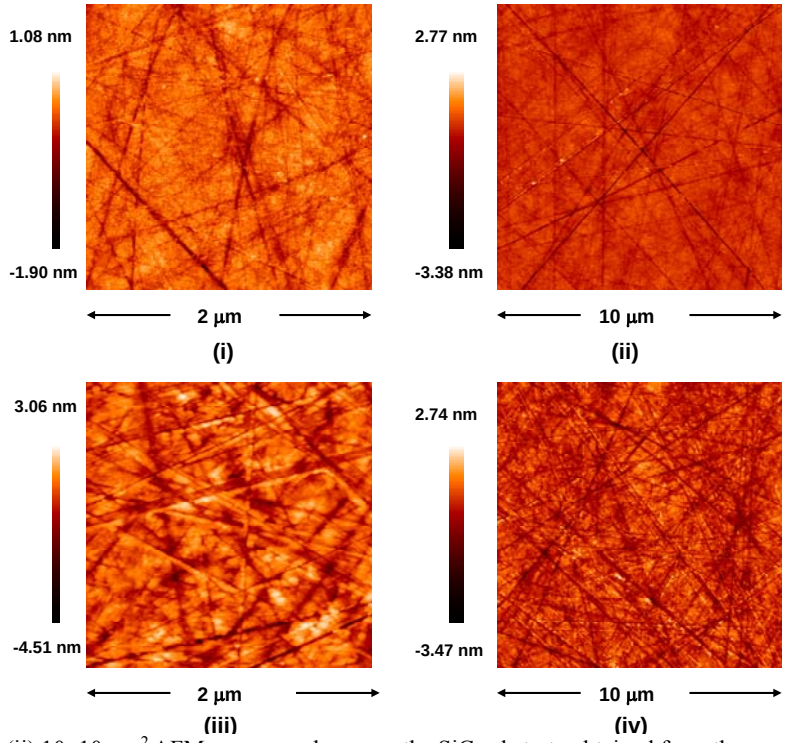

Figure 4: (i) 2×2 µm^2 and (ii) 10×10 µm^2 AFM scans are shown on the SiC substrate obtained from the candidate vendor using polishing process 1 (iii) 2×2 µm^2 and (iv) 10×10 µm^2 AFM scans are shown on the SiC substrate polished using process 2.

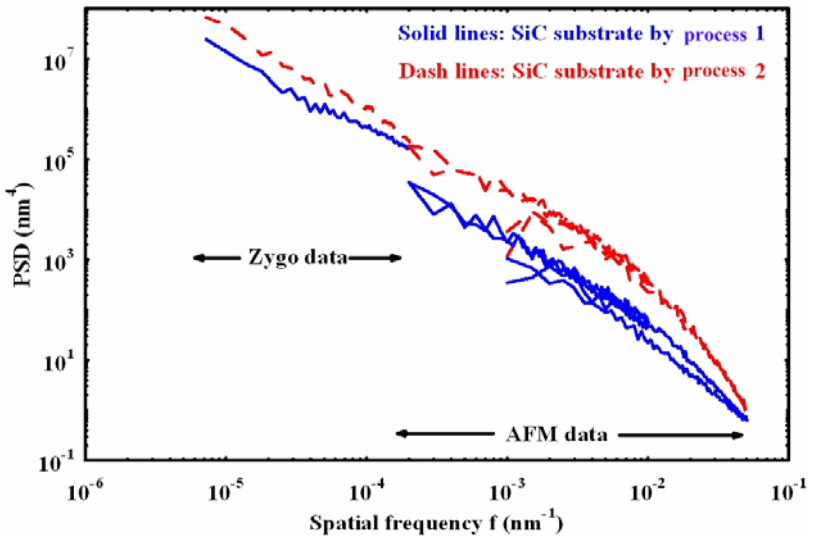

Figure 5: Radially-averaged PSD curves derived from the AFM and Zygo measurements on SiC substrates polished with two different processes.

	Primary Mirror σ (nm RMS)	**Secondary Mirror** σ (nm RMS)
Process 1	0.35	0.30
Process 2	0.90	0.84

Table 4. The high-spatial frequency roughness σ is computed from the PSD curves plotted in Figure 5 in the high-spatial frequency ranges relevant to the primary and secondary HiLiTE mirrors, defined in Table 2.

Deposition of highly reflective multilayer coatings is required on the mirror substrates in order to enable EUV imaging at near-normal angles of incidence. In recent years, there has been significant activity in the area of multilayer coatings operating in the 460 Å wavelength region, due to the advancement of tabletop X-ray lasers[14] and compact, terawatt laser source facilities[15] emitting at 469 Å. Scandium/silicon (Sc/Si)[16,17], and magnesium/silicon carbide (SiC/Mg)[18,19] multilayers have been proposed for normal-incidence imaging in the wavelength region 25-50 nm. Tri-layer multilayers (SiC/Sc/Mg) were proposed more recently for optimized performance[20]. Figure 6 shows experimental results from Mg/SiC multilayers deposited at LLNL, optimized for peak reflectance at 465 Å which is the wavelength of interest for the HiLiTE mission. The samples in Figure 6 were deposited on Si wafer substrates with (100) orientation and < 0.1 nm RMS high-spatial frequency roughness, in a DC-magnetron sputtering system which has been described in detail earlier[21]. Base pressure was maintained at 10^{-7} Torr during the deposition run, and the process gas (Ar) pressure was 10^{-3} Torr. The EUV reflectance results shown in Figure 6 were measured at beamline 6.3.2. of the Advanced Light Source (ALS) synchrotron at Lawrence Berkeley National Laboratory (LBNL). The characteristics of the beamline and its reflectometer have been described in detail earlier[22]. The reflectometer uses a Si photodiode detector, with an acceptance angle of 2.4°. All wavelength and reflectance results shown in Figure 6 were obtained within "2σ" error bars of 0.05% and 0.5% relative, respectively, the latter limited by photodiode uniformity. The results in Figure 6 are very promising – the Mg/SiC material pair appears to have the highest experimental reflectance published in the literature in the 465 Å wavelength range. Film stress was also measured at LLNL on the multilayer films shown in Figure 6, using a FLEXUS™ stress-measuring instrument that uses a laser beam to measure the radius of curvature of the substrate before and after coating. Stress was found to be very low (< 150 MPa) on all four samples, which guarantees that this multilayer film will not deform or delaminate when deposited on large-area flight mirrors. Further optimization of multilayer films for the HiLiTE mission is currently underway and will be presented in a future publication.

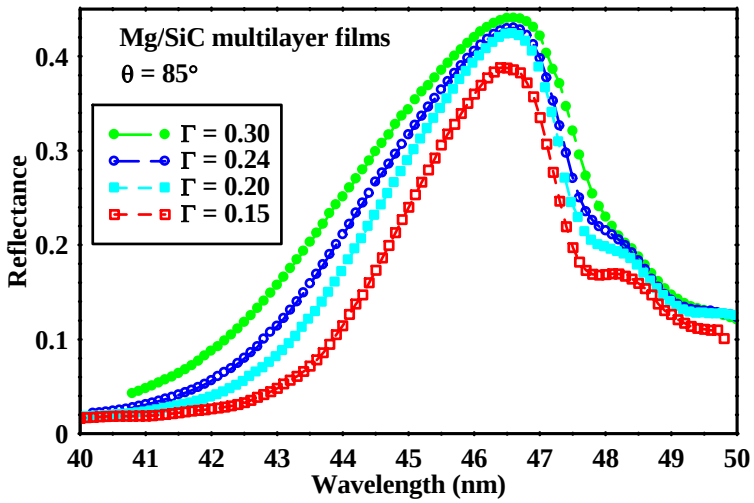

Figure 6: EUV reflectance measurements performed at near-normal incidence angle on four SiC/Mg films are shown. The Γ-value (ratio of SiC thickness inside the SiC/Mg bilayer) is varied among the four multilayer films.

2.3 Expected performance of the HiLiTE telescope in flight

2.3.1. Payload design

The mirrors we will build during the proposed program will be constructed according to the design of the HiLiTE telescope; that is, they will have built-in mounting interfaces that will allow them to be easily integrated into the SiC metering structure. After the completion of this program, in a follow-on program, we will procure the metering structure, and integrate and align the telescope assembly. Additional subsystems that will be required for a rocket flight of the HiLiTE, include thin-film aluminum filters such as those made by Luxel and flown on EIT, TRACE, Hinode, STEREO, AIA and numerous other missions; HiLiTE will require entrance and focal plane filters. The flight electronics do not pose any new engineering challenges and could be assembled from off-the-shelf components.

For its focal plane assembly, HiLiTE will be able to take advantage of novel detector technologies currently in development. LMSAL is already collaborating with e2v and Sarnoff Imaging on the preparation of Active Pixel Sensor devices through a Lockheed Martin Independent Research & Development (IRAD) program. Our baseline optical design assumes such a CMOS camera, with 5 μm pixels and 60% quantum efficiency in the EUV, for the eventual flight of HiLiTE (Figure 7). The QE estimate is based on our experience working with back-illuminated CCD detectors produced by e2v using a similar process. This high efficiency, coupled with the fast read-out capabilities promised by the CMOS detectors, offers the possibility of extremely high-cadence image sequences. While some technical challenges (including noise and non-uniformity) remain in the CMOS detector development effort, the future of these detectors for astronomical applications is very bright with several companies advancing the technology. A full evaluation of the state of the detector development and the trade-offs involved in different approaches will be conducted during the design phase, in collaboration with the LMSAL IRAD effort on CMOS detectors.

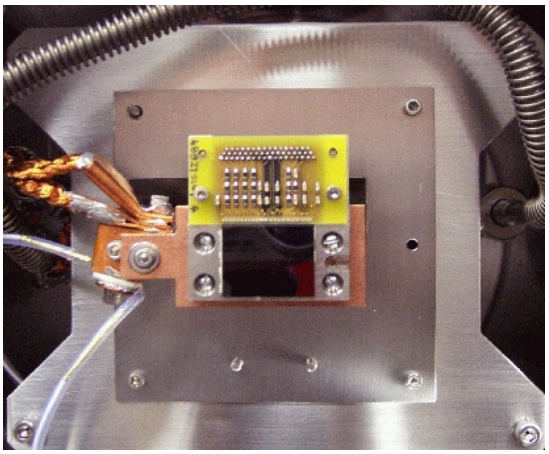

Figure 7. An RAL/e2v, 4k x 3k, 5 μm-pixel active pixel sensor (APS) being tested in the LMSAL IRAD program.

2.3.2 Bandpass and Throughput

In order to achieve the spatial and temporal resolution required to explore the scientific questions raised in the Introduction, we need an effective area sufficient to image 100 photons into an area of the focal plane corresponding to a 0.2 arcsec square column of sight through a typical active region within a 5 second exposure time. This will give us a signal-to-noise ratio of ~10:1 at the finest resolution allowed by the instrument, which is a reasonable threshold based on our experience in the analysis of data from the TRACE mission. This target count rate of 2500 photons/sec/arcsec^2 was used to constrain the size and efficiency of the HiLiTE telescope. We calculated the efficiency of the instrument assuming model multilayer reflectivity and filter transmittance curves. We estimated multilayer reflectivity at ~35% for the primary and secondary, which is a conservative estimate given the results of Figure 6. We then simulated the spectral intensity of a solar active region using APEC[23] and CHIANTI[24], and folded this spectrum through the instrument response to get the count rate as a function of the geometrical collecting area of the telescope. This simulation predicts 13.9 photons/sec/arcsec^2/cm^2 flux entering the telescope aperture. Thus, a 30 cm diameter optic with 80% open area (allowing for spider and secondary mirror obstruction) would detect 13.9 x 565 ~ 7850 photons from an observed 1x1 arcsec^2 area in a 1 sec exposure - more than 3 times our target count rate of 2500 photons/sec/arcsec^2. This simple simulation ignores two significant effects. First, the solar spectrum was simulated using a differential emission measure (DEM) derived from Skylab observations of a number of active regions, broadly averaged in time and space[25]. Of course, active regions are highly structured on small spatial scales, so we can expect a likely enhancement of a factor of ~5 over "average" active region intensity levels for the brightest resolution elements within a HiLiTE image.

This enhancement is partially offset by the second effect of contamination, particularly by hydrocarbons, which can deposit on optical surfaces and which absorb strongly at EUV wavelengths. The wavelength range that includes the 465 Å line is particularly sensitive to this contamination, and the throughput will be attenuated depending on the amount of contaminants on the mirror, filter and detector surfaces. Because of this, we will institute a contamination control plan to minimize the exposure of optical surfaces to hydrocarbons, and will monitor the reflectivity of multilayer witness samples coated before the flight optics to track the buildup of contamination. The contamination control approach will

build on the experience with TRACE, STEREO/SECCHI, SDO/AIA and GOES-R/SUVI at LMSAL. This approach was used successfully on TRACE, where the optics have lost no measurable efficiency due to contamination. We will use low out-gassing materials, and the instrument will be purged with dry nitrogen during assembly and ground operations. If the witness samples show significant contamination, we will consider vacuum baking before an eventual launch.

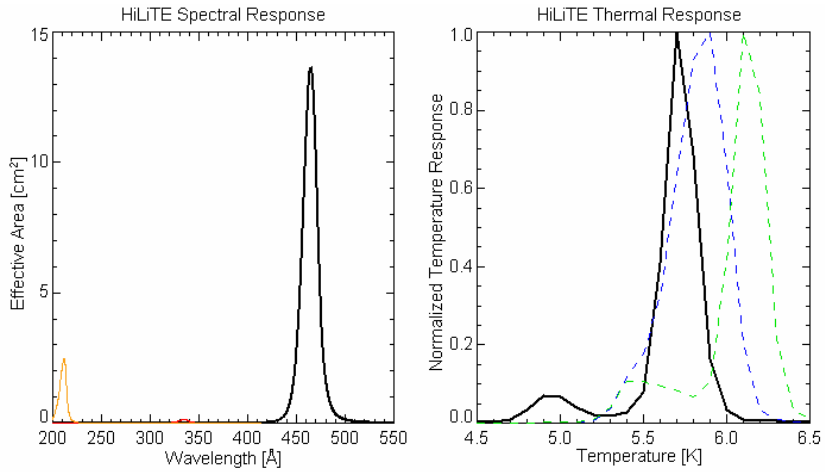

Figure 8. The spectral response of HiLiTE (left) shows the excellent reflectance that can be achieved at 465 Å. The 211 Å (yellow) and 335 Å (red) channels of AIA are shown for comparison. On the right, the thermal response of HiLiTE is shown (black), with a peak at 500,000 K. This temperature range has not yet been accessed by high-resolution EUV multilayer imagers. Also shown are temperature response functions of AIA 171 Å (blue) and 193 Å (green).

Given the allowance for contamination in the throughput budget of HiLiTE, a 30 cm optic should be capable of meeting our minimum count rate goal with a margin of >3x. The spectral response of the instrument model assuming a 30 cm aperture is shown in Figure 8, along with a thermal response calculated with APEC. The temperature response is dominated by Ne VII emission. There is also a weak Ca IX line in the bandpass that contributes ~5% to the total counts, but its formation temperature is so similar to that of Ne VII that the instrument temperature response is still narrow. The multilayers have very low reflectivity at higher orders due to the absorption by the spacer layer, so order-suppressing filters are not required.

2.3.3 Spatial Resolution

The resolution of the assembled HiLiTE telescope will be limited by the stackup of alignment and fabrication errors, as summarized in the preliminary error budget shown in Table 5. Note that the telescope assembly alone will have an in-band resolution of 0.15 arcseconds. Because testing the optical performance of the instrument in the EUV is impractical, this figure will be verified using techniques similar to those employed in the alignment and test of SDO/AIA. Interferometry of the primary and secondary mirrors will be performed after coating and mounting of the optics. Surface maps deduced from these measurements will be used in a ray-trace model of the system, which will also include estimates of the decenter, defocus and tilt of the optics. The resolution will then be measured in autocollimation using a test target illuminated at 450 nm and placed at the focal plane of the telescope. The resolution measurements will be limited by diffraction to ~0.8 arcseconds; however, by measuring the diffraction-limited resolution at different positions in the focal plane and comparing these measurements with the predictions of the model, we will be able to estimate the in-band performance of the instrument. In flight, the resolution of the HiLiTE will be affected by thermal and mechanical shifts induced by launch, and by jitter from the payload pointing system. Fine-pointing of the payload will be accomplished by the digital SPARCS (Solar Pointing Attitude Rocket Control System) system, which is capable of stabilizing the payload to 0.08 arcseconds RMS (Figure 9). These contributions are summarized in the second part of Table . The encircled energy predicted by a Monte Carlo simulation of these error terms using ZEMAX is shown in Figure 10.

	Tolerance	Effect on RMS Spot diameter [μm] Sensitivity	Contribution	Resolution [arcsec]
Initial Primary-Secondary Misalignment				
Decenter	0.1 mm	6 μm/mm	0.60	
Tilt	0.01 deg	200 μm/deg	2.00	
Axial despace of detector	0.1 mm	29 μm/mm	2.90	
Figure errors in coated, mounted optics				
Primary	λ/40 RMS	[analysis]	5.80	
Secondary	λ/40 RMS	[analysis]	2.80	
Optical Design	1.2 μm	1	1.20	
Telescope Assembly Resolution			**7.46**	**0.15**
In-flight Primary-Secondary Misalignment				
Decenter	0.5 mm	6 μm/mm	3.00	
Tilt	0.025 deg	200 μm/deg	5.00	
Axial despace of detector	0.25 mm	29 μm/mm	7.25	
Pointing Jitter	0.08 arcsec	50 μm/arcsec	4.00	
Detector Pixelization	0.08 arcsec	50 μm/arcsec	4.00	
Flight Instrument Resolution			**12.71**	**0.25**

Table 5. Resolution error budget for the HiLiTE telescope in test and flight conditions. Axial despace of the primary and secondary mirrors will be taken up during assembly by despace of the detector. Note that testing at visible-light wavelengths will be limited to a resolution of 0.76 arcseconds.

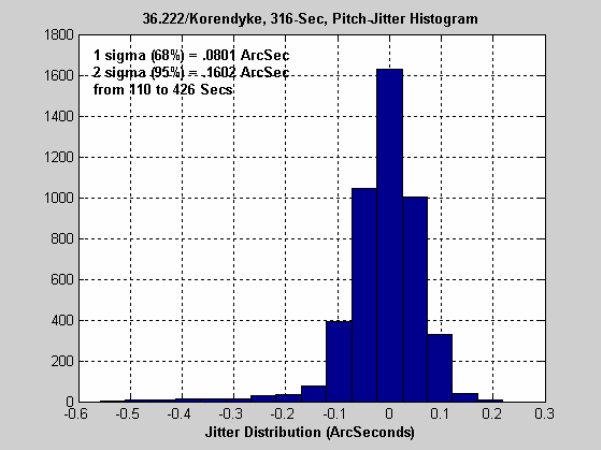

Figure 9: Histogram of pointing data from a recent sun-pointing mission demonstrates that the SPARCS system can achieve pointing stability of 0.08 arcseconds (1-σ).

3. CONCLUSIONS

We have demonstrated the feasibility of the HiLiTE mission, a SiC-based Cassegrain telescope designed to operate at the 465 Å Ne VII emission line, formed in the solar transition region plasma at ~500,000 K. The novel instrument technologies proposed for HiLiTE will open up a new era of Explorer-class missions using large EUV optics.

ACKNOWLEDGEMENTS

We are thankful to Andy Aquila (LBNL) for enlightening discussions and to Julia Meyer-Ilse (LBNL) for assistance with the EUV reflectance measurements. This work was performed under the auspices of the U.S. Department of Energy by Lawrence Livermore National Laboratory under Contract No. DE-AC52-07NA27344, by the University of California Lawrence Berkeley National Laboratory under Contract No. DE-AC03-76F00098 and by Lockheed Martin's Independent Research & Development program.

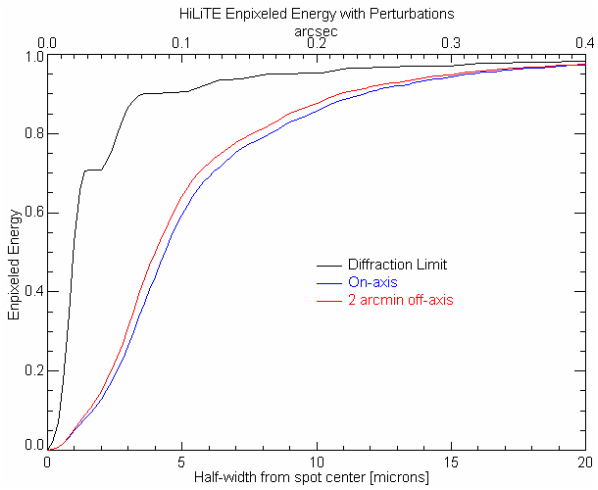

Figure 10. Encircled energy of HiLiTE at various off-axis field angles, based on a Monte Carlo simulation of deformations and misalignments on the order expected during flight on a sounding rocket payload.

REFERENCES

[1] D. S. Martínez-Galarce, P. F. Boerner, S. Deiker, A. Rausch, N. Katz, L. Shing, D. Franks, J. Mix, J. Olson, W. B. Doriese, C. Reintsema, K. Irwin, B. Cabrera, S. W. Leman, T. W. Barbee, P. C. Baker & D. McCammon, "Simulated Soft X-ray Specral Observations with the ATSSI Sounding Rocket Payload", American Astronomical Society, SPD meeting #37, #37.05 (2006).

[2] C. Kankelborg, private communication (2007).

[3] J. Robichaud,, J. Schwartz, D. Landry, W. Glenn, B. Rider, M. Chung, "Recent advances in reaction bonded silicon carbide optics and optical systems", in *Optical Materials and Structures Technologies II*; W. A. Goodman, ed., Proc. SPIE **5868**, 9-15 (2004).

[4] H. Kaneda, T. Nakagawa, K. Enya, T. Onaka, "Cryogenic optical testing of SiC mirrors for ASTRO-F and C/SiC composite mirrors for SPICA", in *Proceedings of the 5th International Conference on Space Optics* (ICSO 2004), B. Warmbein, ed., ESA SP-554, 699 – 706 (2004).

[5] M. Fruit, P. Antoine, J.-L. Varin, H. Bittner, M. Erdmann, "Development of the SOFIA silicon carbide secondary mirror", in *Airborne Telescope Systems II*, R. K. Melugin, H-P Roeser, eds., Proc. SPIE **4857**, 274-285 (2003).

[6] S. J. Conard, F. Azad, *et al.*, "Design and fabrication of the New Horizons Long-Range Reconnaissance Imager", Proc. SPIE, **5906**, 407 (2005).

[7] A. B. C. Walker, Jr., J. F. Lindblom, R. H. O'Neal, M. J. Allen, T. W. Barbee, Jr. & R. B. Hoover, "Multi-Spectral Solar Telescope Array", Opt. Eng. **29**, 581-591 (1990).

[8] D. S. Martínez-Galarce, A. B. C. Walker, D. B. Gore, C. C. Kankelborg, R. B. Hoover, T. W. Barbee, Jr. & P. F. X. Boerner, "High resolution imaging with multilayer telescopes: resolution performance of the MSSTA II telescopes", Opt. Eng. **39**, 1063-1079 (2000).

[9] E. M. Gullikson, "Scattering from normal incidence EUV optics", in *Emerging Lithographic Technologies II*, Y. Vladimirsky, ed.,Proc. SPIE **3331**, 72-80 (1998).

[10] D. G. Stearns, "Stochastic model for thin film growth and erosion," Appl. Phys. Lett. **62**, 1745-1747 (1993).

[11] E. Spiller, S. Baker, E. Parra, and C. Tarrio, "Smoothing of mirror substrates by thin film deposition," in *EUV, X-ray and Neutron Optics and Sources*, C. A. MacDonald, K. A. Goldberg, J. R. Maldonado, H. H. Chen-Mayer, and S. P. Vernon, eds., Proc. SPIE **3767**, 143-153 (1999).

[12] R. Soufli, E. Spiller, M. A. Schmidt, J. C. Robinson, S. L. Baker, S. Ratti, M. A. Johnson and E. M. Gullikson, "Smoothing of diamond-turned substrates for extreme-ultraviolet illuminators", Opt. Eng. **43**, 3089-3095 (2004).

[13] R. Soufli, S. L. Baker, D. L. Windt, J. C. Robinson, E. M. Gullikson, W. A. Podgorski, L. Golub, "Atomic force microscopy characterization of Zerodur mirror substrates for the extreme ultraviolet telescopes aboard NASA's Solar Dynamics Observatory", Appl. Opt. **46**, 3156-3163 (2007).

[14]C. D. Macchietto, B. R. Benware, J.J. Rocca, "Generation of millijoule-level soft-x-ray laser pulses at a 4-Hz repetition rate in a highly saturated tabletop capillary discharge amplifier", Opt. Lett. **24**, 1115-1117 (1999).
[15] J. Dunn, R.F. Smith, J. Nilsen, H. Fiedorowicz, A. Bartnik, V.N. Shlyaptsev, "Picosecond-laser-driven gas puff neonlike argon x-ray laser", J. Opt. Soc. Am. B **20** 203- 207 (2003).
[16] Yu. A. Uspenskii, V.E. Levashov, A. V. Vinogradov, A. I. Fedorenko, V. V. Kondratenko, Yu.P. Pershin, E. N. Zubarev, and V. Yu. Fedotov, "High-reflectivity multilayer mirrors for a vacuum-ultraviolet interval of 35-50 nm", Opt. Lett. **23**, 771-773 (1998).
[17] Yu. A. Uspenskii, J. F. Seely, N. L. Popov, A. V. Vinogradov, Yu. P. Pershin and V. V. Kondratenko, "Efficient method for the determination of extreme ultraviolet optical constants in reactive materials: application to scandium and titanium", J. Opt. Soc. Am. A **21**, 298-305 (2004).
[18] Y. Kondo, T. Ejima, K. Saito, T. Hatano, M. Watanabe, "High reflection multilayer for wavelength range of 200-30 nm", Nucl. Instrum. Meth. Phys. Res. A, **467-468,** 333-336 (2001)
[19] H. Takenaka, S. Ichimaru, T. Ohchi, E.M. Gullikson, "Soft-X-ray reflectivity and heat resistance of SiC/Mg multilayer", J. Electron Spectroscopy and Related Phenomena **144–147** 1047–1049 (2005).
[20] A. Aquila, F. Salmassi, and E.M. Gullikson, "Progress in large period multilayer coatings for high harmonic and solar applications", presented at *the 9th International Conference on the Physics of X-Ray Multilayer Structures (PXRMS)*, Montana, February 3-7, 2008.
[21] R. Soufli, R. M. Hudyma, E. Spiller, E. M. Gullikson, M. A. Schmidt, J. C. Robinson, S. L. Baker, C. C. Walton, and J. S. Taylor "Sub-diffraction-limited multilayer coatings for the 0.3 numerical aperture micro-exposure tool for extreme ultraviolet lithography", Appl. Opt. **46**, 3736-3746 (2007).
[22] E. M. Gullikson, S. Mrowka, B. B. Kaufmann, "Recent developments in EUV reflectometry at the Advanced Light Source," in *Emerging Lithographic Technologies V*, E. A. Dobisz ed., Proc. SPIE **4343**, 363-373 (2001).
[23] R. K. Smith, N. S. Brickhouse, D. A. Liedahl and J. C. Raymond, "Collisional Plasma Models with APEC/APED: Emission-Line Diagnostics of Hydrogen-like and Helium-like Ions", Astrophysical Journal **556,** L91-L95 (2001).
[24] P. R. Young, G. Del Zanna, E. Landi, K. P. Dere, H. E. Mason, M. Landini, "CHIANTI - An Atomic Database for Emission Lines. VI. Proton Rates and Other Improvements", Astrophysical Journal Supp. Series **144 (1),** 132-152 (2003).
[25] J. E. Vernazza and E. M. Reeves, "Extreme ultraviolet composite spectra of representative solar features", Astrophysical Journal **37,** 485-513 (1978).